Feynman-Smoluchowski ratchet in an effective one-dimensional picture

Pavol Kalinay[1] and František Slanina[2]
[1]*Institute of Physics, Slovak Academy of Sciences, Dúbravska cesta 9, 84511 Bratislava, Slovakia*
[2]*Institute of Physics, Academy of Sciences of the Czech Republic, Na Slovance 2, CZ-18221 Praha, Czech Republic*

(Received 28 June 2018; published 25 October 2018)

A simple two-dimensional (2D) model of the Feynman-Smoluchowski ratchet is studied. Motion of the wheel, driven by stochastic hits of the surrounding molecules, is described as diffusion along the longitudinal coordinate x; the stochastic motion of the pawl is represented in the transverse coordinate y. Different temperatures of the reservoirs connected to the particular degrees of freedom, together with asymmetry of the energetic landscape of the system, give rise to the ratchet effect. We apply mapping of the corresponding 2D Fokker-Planck equation onto the longitudinal coordinate x. The mapped 1D equation is of the generalized Fick-Jacobs type with an effective potential containing a part increasing or decreasing with x, connected with vorticity of the scaled driving force and the stationary probability current. It is responsible for the final rectified motion in the longitudinal direction.

DOI: 10.1103/PhysRevE.98.042141

I. INTRODUCTION

One of the best-known devices invented to demonstrate (im)possibility to gain work from the thermal motion of molecules was suggested by Smoluchowski [1] as a thought experiment 100 years ago. It consists of a ratchet wheel connected to an axle with paddles [2]. Molecules of the surrounding gas hit the paddles from both sides, rotating the wheel stochastically in both directions. The random motion of the wheel is intended to be rectified by use of a pawl, protecting the wheel to rotate in one ("backward") direction.

The described device does not work, as the pawl capable of reacting to single hits of the molecules has to be microscopic, too. Its position (height) with respect to the wheel is stochastic as well, influenced by the (spring) force pushing the pawl to the wheel and also its temperature. Combination of both stochastic motions results in no net rectified motion of the wheel, i.e., no used energy of the thermal motion of the surrounding gas.

Still, Feynman showed [3] that the wheel should prefer moving in one direction if both the gas surrounding the paddles and the pawl are connected to reservoirs of different temperatures. Of course, in this case, the device becomes a kind of a heat engine, the thermal ratchet [2], changing the thermal energy flowing from the hot reservoir to the cold one through the ratchet to the mechanical work done on the rotating wheel.

Mathematically, the system can be described as a two-dimensional (2D) diffusion in a specific potential landscape. The longitudinal coordinate x corresponds to the angle of the rotating wheel; the transverse coordinate y represents the height of the pawl. The potential $U(x, y)$ is given by the strength of the spring pushing the pawl to the wheel and also the angle of the ratchet wheel x. In the simplest case, the motion of the wheel and the pawl can be considered viscous, in the overdamped limit, so the probability density of the system $\rho(x, y, t)$ being in the position (x, y) at time t evolves according to the Fokker-Planck equation

$$\partial_t \rho(x, y, t) = [D_x \partial_x e^{-\beta_x U(x,y)} \partial_x e^{\beta_x U(x,y)} + D_y \partial_y e^{-\beta_y U(x,y)} \partial_y e^{\beta_y U(x,y)} \rho(x, y, t), \quad (1)$$

$\beta_x = 1/k_B T_x$, $\beta_y = 1/k_B T_y$ are the inverse temperatures of the reservoirs connected to the gas and the pawl, respectively; D_x and D_y denote the diffusion constants in the corresponding directions. If the temperatures $T_x = T_y$, Eq. (1) becomes the Smoluchowski equation, describing diffusion in the potential $U(x, y)$ with no ratchet effect.

The crucial property of the potential is its asymmetry, $U(x, y) \neq U(-x, y)$ for any choice of the origin of the coordinate x, reflecting asymmetry of the teeth of the ratchet wheel. To show only functionality of the Feynman-Smoluchowski ratchet, we may modify the real potential $U(x, y)$ in a way making our analysis easier, preserving its asymmetry. Ryabov *et al.* [4,5] succeeded to express the leading term of the rectified velocity in the x direction (and the related quantities) using the potential harmonic in the y coordinate, $U(x, y) = k(x)y^2$. It mimics the teeth of the ratchet by asymmetric spring constant $k(x) \neq k(-x)$, depending on x. In the presented works, the scaling of the transverse diffusion constant was used and the homogenization method up to the first order was applied, similar to the mapping of diffusion in a 2D channel onto the longitudinal coordinate [6–9] calculated in the stationary regime [10].

Recently, this mapping procedure was generalized to projection of the 2D advection-diffusion equation

$$\partial_t \rho(x, y, t) = D_x \left[\partial_x (\partial_x - f(x, y)) + \frac{1}{\epsilon} \partial_y (\partial_y - g(x, y)) \right] \rho(x, y, t) \quad (2)$$

onto the x coordinate [11] for an arbitrary driving force $(f(x, y), g(x, y))$ (rescaled by an inverse temperature $1/k_B T$), also including the nonconservative forces. Despite

of non existing scalar potential in this case, the result of the mapping is again the 1D Fick-Jacobs (FJ) equation [12],

$$\partial_t p(x,t) = D_x \partial_x A(x) \partial_x \frac{p(x,t)}{A(x)}, \tag{3}$$

generalized by a series of corrections $\hat{Z}_n(x,\partial_x)$, controlled by the small parameter ϵ,

$$\partial_t p(x,t) = D_x \partial_x A(x) \left[1 - \sum_{n=1}^{\infty} \epsilon^n \hat{Z}_n(x,\partial_x) \right] \partial_x \frac{p(x,t)}{A(x)}. \tag{4}$$

It governs the marginal (1D) probability density

$$p(x,t) = \int_{\sigma(x)} \rho(x,y,t) dy; \tag{5}$$

the integration goes over the local cross-section $\sigma(x)$. If the driving force is conservative, i.e., $f(x,y) = -\partial_x U(x,y)/k_B T$, $g(x,y) = -\partial_y U(x,y)/k_B T$, the function $A(x) = \int_{\sigma(x)} e^{-U(x,y)/k_B T} dy$ is a local partition function [9] at a fixed x. The mapping of Eq. (2) with a nonconservative force (f,g) showed that, also in this case, the function $A(x)$ can be consistently defined.

Still, there are some peculiarities of the corresponding 1D picture, if compared with the generalized FJ equation for diffusion alone. Validity of Eq. (4) means that also a (quasi-) equilibrium with the 1D density $p_{\rm eq}(x) \sim A(x)$ exists. The analysis [11] shows that although the quasiequilibrium densities $p_{\rm eq}$, $\rho_{\rm eq}$ are constant in time, the nonconservative force drives a nonzero stationary flux circulating in the channel. The function $A(x)$ also becomes dependent on the parameter ϵ; its higher-order corrections can give nontrivial contributions to the standard entropic potential.

The effective 1D theory based on the mapping of Eq. (2) was aimed mainly to describe a confined diffusion of particles under hydrodynamical drag [13–15]. Nevertheless, Eq. (1) can be easily converted to Eq. (2), identifying $f(x,y) = -\beta_x \partial_x U(x,y)$, $g(x,y) = -\beta_y \partial_y U(x,y)$ and $\epsilon = D_x/D_y$, so the theory can be used for description of the Feynman-Smoluchowski ratchet as well. Besides, for different temperatures of the reservoirs, $\beta_x \neq \beta_y$, the scaled force (f,g) becomes nonconservative and the peculiarities of the 1D theory mentioned above, related to existence of the stationary circulating (vortex) probability currents appearing in the corresponding 2D picture, may become the key helping to understand functionality of the ratchet.

The purpose of this work is to apply the mapping of Eq. (2) and the corresponding Eq. (5) on the Feynman-Smoluchowski ratchet. From one side, it is a model, which can be treated analytically within a rather complicated effective theory; it represents a useful nontrivial example for it. However, the 1D picture brings a new insight on description how the ratchet works. Our paper consists of two parts. In Sec. II, we revisit the key points of the mapping of Eq. (2). This theory is applied on the Feynman-Smoluchowski ratchet in Sec. III, also analyzing the role of vorticity in breaking periodicity of the 1D effective potential $\sim\epsilon$, causing finally the rectified motion of the ratchet.

II. MAPPING PROCEDURE

We revisit here briefly the mapping of Eq. (2) onto the longitudinal coordinate x, adjusting the procedure [11] for our needs to describe the Feynman-Smoluchowski ratchet in the next section. First, we set the intrinsic diffusion constant $D_x = 1$; it only defines the timescale. Next, we define the integration region $\sigma(x)$ in Eq. (5), corresponding to the possible positions of the pawl. Its lower limit is restricted by the teeth of the ratchet, varying with some function $h(x)$, the upper limit can be set to infinity, as the higher positions y are achieved with vanishing probability due to positive spring constant $k(x)$ for any x. So the transverse coordinate $y \in \sigma(x) = (h(x), \infty)$. Equation (2) is supplemented by the boundary condition (BC),

$$[\partial_y - g(x,y)]\rho(x,y,t)|_{y=h(x)} = \epsilon h'(x)[\partial_x - f(x,y)] \times \rho(x,y,t)|_{y=h(x)}, \tag{6}$$

requiring the normal component of the flux density $\vec{j}$,

$$j_x(x,y,t) = -[\partial_x - f(x,y)]\rho(x,y,t),$$
$$j_y(x,y,t) = -\frac{1}{\epsilon}[\partial_y - g(x,y)]\rho(x,y,t), \tag{7}$$

at the boundary $y = h(x)$ was zero. Notice that unlike Ref. [11], this boundary represents now the lower limit, which results in different signs in several formulas. Also the parameter ϵ is defined by anisotropy of the diffusion constants instead of scaling the transverse lengths; both concepts are mathematically equivalent.

Integration of Eq. (2) over $y \in \sigma(x)$ gives the mapped equation of the form

$$\partial_t p(x,t) = \partial_x \left[\partial_x p(x,t) + h'(x)\rho[x,h(x),t] - \int_{h(x)}^{\infty} f(x,y)\rho(x,y,t) dy \right], \tag{8}$$

having used twice $\int_{h(x)}^{\infty} \partial_x \phi(x,y) dy = \partial_x \int_{h(x)}^{\infty} \phi(x,y) dy + h'(x)\phi(x,h(x))$, valid for any $\phi(x,y)$, and applying the definition Eq. (5) and the BC Eq. (6). The key problem is to express $\rho(x,y,t)$ and its values at $y = h(x)$ using $p(x,t)$ to obtain the equation of the form Eq. (4).

A. Zeroth-order approximation

The first step is always the FJ approximation, supposing that $\epsilon \to 0$, i.e., relaxation of $\rho(x,y,t)$ to the local equilibrium distribution (at a fixed x) in the transverse (y) direction is infinitely fast. For nonconservative forces, there is no scalar potential, but still, one can define a function

$$G(x,y) = -\int_{h_0}^{y} g(x,y')dy' - \gamma(x), \tag{9}$$

such that the zeroth-order 2D density

$$\rho_0(x,y,t) = e^{-G(x,y)} \frac{p(x,t)}{A(x)} \tag{10}$$

has the necessary properties of the relaxed distribution: if substituted in Eq. (2), the singular term $\sim 1/\epsilon$ gives zero and also the BC Eq. (6) for $\epsilon \to 0$ is satisfied. The constant h_0 is an arbitrary reference distance from the x axis; we

only require that $h_0 \geqslant h(x)$ for any x. Consistency with the definition Eq. (5) is ensured by

$$A(x) = \int_{h(x)}^{\infty} e^{-G(x,y)} dy. \tag{11}$$

The function $\gamma(x)$ is a calibration function, which cancels in Eq. (10); its relevance will become obvious later. Our method requires us to expand it in ϵ,

$$\gamma(x) = \sum_{n=0}^{\infty} \epsilon^n \gamma_n(x). \tag{12}$$

Applying Eq. (10) for $\rho(x, y, t)$ in Eq. (8), we obtain

$$\begin{aligned} \partial_t p(x,t) &= \partial_x \Big[\partial_x A(x) + h'(x) e^{-G[x,h(x)]} \\ &\quad - \int_{h(x)}^{\infty} f(x,y) e^{-G(x,y)} dy \Big] \frac{p(x,t)}{A(x)} \\ &= \partial_x A(x) \Big[\partial_x + \frac{A'(x)}{A(x)} + \frac{h'(x)}{A(x)} e^{-G[x,h(x)]} \\ &\quad - \langle f \rangle(x) \Big] \frac{p(x,t)}{A(x)}; \end{aligned} \tag{13}$$

the prime denotes the x derivative and the symbol

$$\langle \phi \rangle(x) = \frac{1}{A(x)} \int_{h(x)}^{\infty} \phi(x,y) e^{-G(x,y)} dy \tag{14}$$

for any function ϕ. Equation (13) can be converted to the FJ form Eq. (3) by fixing the calibration function $\gamma_0(x)$ to eliminate all the terms in the square brackets of Eq. (13) but ∂_x. Expressing the derivative $G'(x, y)$ as

$$\begin{aligned} -G'(x,y) = -\partial_x G(x,y) &= \int_{h_0}^{y} [\partial_x g(x,y') - \partial_{y'} f(x,y') \\ &\quad + \partial_{y'} f(x,y')] dy' + \gamma'(x) \\ &= w(x,y) + f(x,y) - f(x,h_0) + \gamma'(x), \end{aligned} \tag{15}$$

$\gamma_0(x)$, contained in the term

$$\begin{aligned} \frac{A'(x)}{A(x)} &= -\frac{h'(x)}{A(x)} e^{-G[x,h(x)]} - \int_{h(x)}^{\infty} \frac{G'(x,y)}{A(x)} e^{-G(x,y)} dy \\ &= \langle w + f \rangle(x) - f(x,h_0) - \frac{h'(x)}{A(x)} e^{-G[x,h(x)]} \\ &\quad + \sum_{n=0}^{\infty} \epsilon^n \gamma_n'(x) \end{aligned} \tag{16}$$

of Eq. (13), is set by the condition

$$\gamma_0'(x) = f(x,h_0) - \langle w \rangle(x). \tag{17}$$

The higher-order $\gamma_n(x)$ do not influence the obtained zeroth-order FJ equation.

A new function was introduced here, the "vortex force,"

$$w(x,y) = \int_{h_0}^{y} [\partial_x g(x,y') - \partial_{y'} f(x,y')] dy', \tag{18}$$

which is nonzero only for nonconservative force (f, g). The zeroth order of $G(x, y)$,

$$\begin{aligned} G_0(x,y) &= \int [\langle w \rangle(x) - f(x,h_0)] dx - \int_{h_0}^{y} g(x,y') dy' \\ &= G(x,y) + \sum_{n=1}^{\infty} \epsilon^n \gamma_n(x) \end{aligned} \tag{19}$$

represents the (minus) work done by the force f minus an averaged $\langle w \rangle$ along the line $y = h_0$ from some reference point to (x, h_0) and then by the force g to the point (x, y). For the conservative forces, $G_0(x, y)$ becomes the scalar potential $\beta U(x, y)$, $\partial_x G_0(x, y) = -f(x, y)$, $\partial_y G_0(x, y) = -g(x, y)$, consistently with $w(x, y) = 0$ according to the definition Eq. (18). For the nonconservative forces, the x derivative

$$\begin{aligned} -\partial_x G_0(x,y) &= f(x,y) + w(x,y) - \langle w \rangle(x) \\ &= f(x,y) + \Delta w(x,y) \end{aligned} \tag{20}$$

contains an extra contribution from the vortex force $\Delta w = w - \langle w \rangle$. Similar to Eq. (11), we also define

$$A_0(x) = \int_{h(x)}^{\infty} e^{-G_0(x,y)} dy = A(x) e^{-\sum_{n=1}^{\infty} \epsilon^n \gamma_n(x)}. \tag{21}$$

The functions G and A in the transverse averaging, Eq. (14), can be replaced by the ϵ- independent G_0 and A_0, as the exponentials of the higher-order γ_n in the numerator and the denominator cancel one another.

B. Higher-order corrections

Having the zeroth-order (FJ) equation derived, we present the recurrence procedure generating the corrections $\hat{Z}_n$. The true 2D density $\rho(x, y, t)$ is expressed as

$$\rho(x,y,t) = e^{-G(x,y)} \sum_{n=0}^{\infty} \epsilon^n \hat{\omega}_n(x,y,\partial_x) \frac{p(x,t)}{A(x)}; \tag{22}$$

$\hat{\omega}_n(x, y, \partial_x)$ are some operators generating the nth-order corrections to $\rho_0(x, y, t)$, Eq. (10), if applied on any 1D solution $p(x, t)/A(x)$. Consistently with Eq. (10), $\hat{\omega}_0(x, y, \partial_x) = 1$. The higher-order operators are found recursively using the advection-diffusion Eq. (2) with ρ substituted from Eq. (22),

$$\begin{aligned} 0 = \sum_{n=0}^{\infty} \epsilon^n \Big\{ \partial_t - \partial_x [\partial_x - f(x,y)] - \frac{1}{\epsilon} \partial_y [\partial_y - g(x,y)] \Big\} \\ \times e^{-G(x,y)} \hat{\omega}_n(x,y,\partial_x) \frac{p(x,t)}{A(x)}; \end{aligned} \tag{23}$$

the operators of partial derivatives act on anything to the right. Notice that $e^{-G(x,y)} \hat{\omega}_n(x, y, \partial_x) A^{-1}(x)$ does not depend on time, so the time derivative ∂_t commutes with it and acts directly on $p(x, t)$. For $\partial_t p(x, t)$, we apply Eq. (4). Finally, Eq. (23) with purely spatial operators on the right-hand side has to be satisfied for any $p(x, t)/A(x)$, i.e., on the level of operators, in each order of ϵ. Collecting the terms standing

at the same powers of ϵ^n, we obtain recurrence operator equations fixing the higher $\hat{\omega}_n(x, y, t)$ by sequel. Having the next order $\hat{\omega}_n$ calculated, the corresponding $\hat{Z}_n(x, \partial_x)$ is found from Eq. (8) with $\rho(x, y, t)$ expressed using Eq. (22),

$$\partial_t p(x,t) = \partial_x A(x)\Bigg(\partial_x + \sum_{n=1}^{\infty}\epsilon^n\Big\{\gamma_n'(x) + \frac{h'(x)}{A_0(x)}e^{-G_0[x,h(x)]}\hat{\omega}_n[x,h(x),\partial_x] - \langle f\hat{\omega}_n\rangle(x,\partial_x)\Big\}\Bigg)\frac{p(x,t)}{A(x)}; \tag{24}$$

the formulas derived above for the zeroth order have been already used here.

As shown in Ref. [11], the recurrence procedure for the nonconservative forces gives the operators $\hat{\omega}_n$ with nonzero terms not containing ∂_x. They can be split as

$$\hat{\omega}_n(x, y, \partial_x) = \omega_n(x, y) + \tilde{\omega}_n(x, y, \partial_x)\partial_x, \tag{25}$$

where $\omega_n(x, y)$ are just functions. These terms violate the structure of the generalized FJ equation as known from the mapping of diffusion in conservative fields [9]. They can be eliminated in Eq. (24) by setting the calibration function

$$\gamma_n'(x) = \langle f\omega_n\rangle(x) - \frac{h'(x)}{A_0(x)}e^{-G_0[x,h(x)]}\omega_n[x,h(x)]. \tag{26}$$

Then Eqs. (24) and (4) can be compared, giving

$$\hat{Z}_n(x,\partial_x) = \langle f\tilde{\omega}_n\rangle(x,\partial_x) - \frac{h'(x)}{A_0(x)}e^{-G_0[x,h(x)]}\tilde{\omega}_n[x,h(x),\partial_x]. \tag{27}$$

The advection-diffusion Eq. (2) can be mapped onto the generalized FJ Eq. (4) for nonconservative forces, too, for the price that the functions $G(x, y)$ and $A(x)$ become dependent on ϵ and contain the calibration functions $\gamma_n(x)$. It makes the recurrence procedure, calculating $\hat{\omega}_n(x, y, \partial_x)$ noticeably more complicated than for the diffusion alone. We derive here only the first-order correction, giving the leading terms of quantities describing functionality of the ratchet.

Collecting the terms $\sim\epsilon^0$ in Eq. (23), we obtain the operator equation determining $\hat{\omega}_1$,

$$\begin{aligned}&\partial_y[\partial_y - g(x,y)]e^{-G(x,y)}\hat{\omega}_1(x,y,\partial_x)\\ &\quad= [(\partial_t - \partial_x[\partial_x - f(x,y)])]e^{-G(x,y)}\hat{\omega}_0(x,y,\partial_x)\\ &\quad= e^{-G(x,y)}\frac{1}{A(x)}\partial_x A(x)\partial_x - \partial_x[\partial_x - f(x,y)]e^{-G(x,y)},\end{aligned}$$

$\hat{\omega}_0(x, y, \partial_x) = 1$. It acts on (any) $p(x, t)/A(x)$, so ∂_t, commuting with the spatial operator $e^{-G(x,y)}$, is replaced by $A^{-1}(x)\partial_x A(x)\partial_x$, according to the FJ Eq. (3), valid in the zeroth order. Also G and A can be replaced by the zeroth-order functions G_0 and A_0; we obtain

$$\begin{aligned}&\partial_y e^{-G_0(x,y)}\partial_y\hat{\omega}_1(x,y,\partial_x)\\ &\quad= e^{-G_0(x,y)}\left[\frac{A_0'(x)}{A_0(x)} - f(x,y) - 2\Delta w(x,y)\right]\partial_x\\ &\qquad- [e^{-G_0(x,y)}\Delta w(x,y)]'\end{aligned} \tag{28}$$

after some algebra and using Eq. (20). Double integration over y gives

$$\begin{aligned}\hat{\omega}_1(x,y,\partial_x) = \hat{C}_1(x,\partial_x) - \int dy e^{G_0(x,y)}\int_y^{\infty}\Big\{&e^{-G_0(x,y')}\\ &\times\left[\frac{A_0'(x)}{A_0(x)} - f(x,y') - 2\Delta w(x,y')\right]\partial_x\\ &- [e^{-G_0(x,y')}\Delta w(x,y')]'\Big\}dy';\end{aligned} \tag{29}$$

the first integration constant has to provide convergence of the result in $y \to \infty$, the second one, $\hat{C}_1(x, \partial_x)$, is set to satisfy consistency of Eq. (5),

$$p(x,t) = \sum_{n=0}^{\infty}\epsilon^n\int_{h(x)}^{\infty}dy e^{-G(x,y)}\hat{\omega}_n(x,y,\partial_x)\frac{p(x,t)}{A(x)}, \tag{30}$$

for any 1D solution $p(x, t)$ in any order of ϵ, hence we get $\langle\hat{\omega}_n\rangle(x, \partial_x) = 0$ for $n > 0$. Of course, $\hat{C}_n$ is constant in y, but it is an operator in x.

The result Eq. (29) demonstrates the structure of $\hat{\omega}_1$ described above. Aside from the term proportional to ∂_x, which is standard in the mapping of diffusion or in a scalar field, there is a new term not containing ∂_x, appearing here for a nonzero vortex force w. To obtain the mapped equation of the form Eq. (4), $\gamma_1(x)$ is fixed according to Eq. (26), then $\hat{Z}_1$ is expressed from Eq. (27).

Collecting the terms standing at higher powers of ϵ, to get equations for $\hat{\omega}_2$, etc., requires us also to expand $e^{-G(x,y)}$ and $A(x)$ in Eqs. (23) and (4), making the equations like Eq. (28) much more complicated. A rather compact formulation enabling us to apply the projection in the higher orders, too, was suggested in Ref. [11].

Validity of Eq. (4) means, that an effective potential $U_{\rm eff}(x) = -k_B T \ln A(x)$ in the 1D picture can be defined, despite of non existing 2D scalar potential for nonzero vortex forces. Then a quasiequilibrium is found, with $p_{\rm eq}(x)/A(x) =$ const., as well as a stationary flow, given by a nonzero net flux

$$\begin{aligned}J &= \int_{h(x)}^{\infty} j_x(x,y)dy\\ &= A(x)\left[1 - \sum_{n=1}^{\infty}\epsilon^n\hat{Z}_n(x,\partial_x)\right]\frac{p_{st}(x)}{A(x)},\end{aligned} \tag{31}$$

constant in time and space. The quasiequilibrium exhibits peculiarities for the nonconservative forces; the backward mapped 2D density

$$\rho_{\rm st}(x,y) \sim e^{-G(x,y)}\left[1 + \sum_{n=1}^{\infty}\epsilon^n\omega_n(x,y)\right], \tag{32}$$

calculated according to Eqs. (22) and (25), does not have the form of Gibbs distribution. Using it in Eq. (7), the flux density

$$j_x(x,y) \sim e^{-G(x,y)}\left[\sum_{n=1}^{\infty}\epsilon^n \partial_x \omega_n(x,y) + \left(\Delta w(x,y) + \sum_{j=1}^{\infty}\epsilon^j \gamma_j'(x)\right)\sum_{n=0}^{\infty}\epsilon^n \omega_n(x,y)\right],$$

$$j_y(x,y) \sim -\frac{1}{\epsilon}e^{-G(x,y)}\sum_{n=1}^{\infty}\epsilon^n \partial_y \omega_n(x,y), \tag{33}$$

appears nonzero for $w(x,y) \neq 0$. The nonconservative forces drive stationary circulating currents in the quasiequilibrium [11], giving the zero net flux, Eq. (31). A similar picture is also observed for stationary flow, only J is nonzero.

In the next section, we apply this theory on a model of the Feynman-Smoluchowski ratchet. The peculiarities appear to be related closely to its functionality. In the 1D picture, the functions $\gamma_n(x)$ become corrections to the effective potential, which brake periodicity of the system and drive it in one direction.

III. RYABOV'S MODEL

We apply here the effective 1D theory to the model of Ryabov *et al.* [4,5]. The lower boundary $h(x) = 0$, hence the parameter $h_0 = 0$ can also be used. The effect of asymmetric teeth of the ratchet wheel is modeled by a spring constant $k(x)$, varying with position of the wheel, i.e., the longitudinal coordinate x. The landscape is given by the potential $U(x,y) = k(x)y^2$.

Due to different temperatures T_x and T_y, the scaled force

$$f(x,y) = -\beta_x \partial_x U(x,y) = -\beta_x k'(x) y^2,$$
$$g(x,y) = -\beta_y \partial_y U(x,y) = -2\beta_y k(x) y, \tag{34}$$

obtained from Eq. (1), becomes nonconservative. According to the definition Eq. (18), the vortex force

$$w(x,y) = (\beta_x - \beta_y)k'(x)y^2 \tag{35}$$

is nonzero, proportional to the difference of temperatures $T_y - T_x$. The functions $G(x,y)$ and $A(x)$ are

$$G(x,y) = \beta_y k(x) y^2 - \gamma(x),$$
$$A(x) = \sqrt{\frac{\pi}{4\beta_y k(x)}}\, e^{\gamma(x)}, \tag{36}$$

with an unknown yet calibration function $\gamma(x)$. It does not prevent us from expressing the transverse average

$$\langle w\rangle(x) = \frac{(\beta_x - \beta_y)k'(x)}{2\beta_y k(x)} \tag{37}$$

unambiguously according to Eq. (14), as the exponentials $e^{\gamma(x)}$ in e^{-G} and A are canceled.

To obtain the zeroth-order FJ equation, the $\gamma_0(x)$ is fixed from Eq. (17),

$$\gamma_0'(x) = f(x,0) - \langle w\rangle(x) = -\frac{(\beta_x - \beta_y)k'(x)}{2\beta_y k(x)}. \tag{38}$$

After integration over x (with an irrelevant integration constant), we find the zeroth-order functions

$$G_0(x,y) = \beta_y k(x) y^2 + \frac{(\beta_x - \beta_y)}{2\beta_y}\ln k(x),$$
$$A_0(x) = \sqrt{\pi/4\beta_y}\; k^{-\beta_x/2\beta_y}(x); \tag{39}$$

the last one enters the FJ Eq. (3).

The ratchet effect appears in the first-order correction [4,5], so we continue to calculate $\hat{\omega}_1$, $\hat{Z}_1$, and γ_1 to find its leading contribution. Substituting for f, g, and $\Delta w = w - \langle w\rangle$ in Eq. (28) from the relations Eqs. (34)–(37), we derive

$$\partial_y e^{-G_0}\partial_y \hat{\omega}_1 = e^{-G_0}\left\{\left(1 - \frac{\beta_x}{2\beta_y}\right)\frac{k'}{k}(2\beta_y k y^2 - 1)\partial_x + \left(\frac{\beta_x}{\beta_y} - 1\right)\left[\frac{k'^2}{k^2}\left(\beta_y^2 k^2 y^4 + \frac{\beta_x - 2\beta_y}{2}ky^2 - \frac{\beta_x + \beta_y}{4\beta_y}\right) - \frac{k''}{2k}(2\beta_y k y^2 - 1)\right]\right\} \tag{40}$$

(omitting the obvious arguments). Double integration over y according to Eq. (29) can be completed analytically; it results in $\hat{\omega}_1$ of the form Eq. (25). Both parts,

$$\tilde{\omega}_1(x,y) = \frac{(\beta_x - 2\beta_y)k'}{4\beta_y k}\left(y^2 - \frac{1}{2\beta_y k}\right),$$
$$\omega_1(x,y) = \frac{(\beta_y - \beta_x)}{8\beta_y}\left[\frac{k'^2}{k^2}\left(\beta_y k y^4 + \frac{\beta_x + \beta_y}{\beta_y}y^2 - \frac{2\beta_x + 5\beta_y}{4\beta_y^2 k}\right) - \frac{2k''}{k}\left(y^2 - \frac{1}{2\beta_y k}\right)\right], \tag{41}$$

have the y-independent terms fixed to satisfy the normalization condition Eq. (30). Then the corrections γ_1 and $\hat{Z}_1$ are calculated using Eqs. (26) and (27),

$$\gamma_1'(x) = \frac{(\beta_x - \beta_y)\beta_x k'(x)}{8\beta_y^3 k^2(x)}\left[\frac{(\beta_x + 4\beta_y)k'^2(x)}{2\beta_y k^2(x)} - \frac{k''(x)}{k(x)}\right],$$
$$\hat{Z}_1(x) = \frac{(2\beta_y - \beta_x)\beta_x k'^2(x)}{8\beta_y^3 k^3(x)}. \tag{42}$$

Notice that if $\beta_x = \beta_y$, the formulas for $A_0(x)$, $\hat{\omega}_1(x,y,\partial_x)$ and $\hat{Z}_1(x,\partial_x)$ reproduce the corresponding relations for the mapped Smoluchowski equation [9], taking $\alpha(x) = \beta_y k(x)$. The functions $\omega_1(x,y)$ and $\gamma_1(x)$, proportional to the difference $(\beta_x - \beta_y)$ are new here; we show that they are responsible for appearance of the ratchet effect. The integral of $\gamma_1'(x)$, Eq. (42),

$$\gamma_1(x) = \frac{\beta_x(\beta_x - \beta_y)}{16\beta_y^3}\left[\left(1 + \frac{\beta_x}{\beta_y}\right)\int \frac{k'^3(x)}{k^4(x)}dx - \frac{k'^2(x)}{k^3(x)}\right], \tag{43}$$

can also break periodicity of the system; for some periodic $k(x) = k(x+L)$, the primitive function in Eq. (43) exhibits a nonzero increment over one period L. The function $\gamma_1(x)$ represents the first-order correction of $G(x,y)$ and $\ln A(x)$, i.e., the effective (entropic + real) 1D potential. The nonzero increment over L makes it a slanted washboard potential,

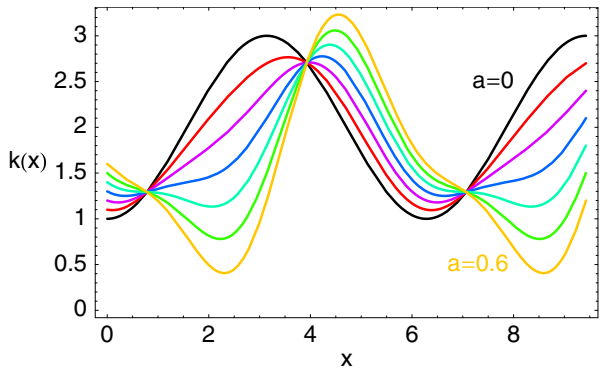

FIG. 1. The spring stiffness $k(x)$ according to Eq. (44) ordered consecutively for $a = 0$ (black), 0.1 (red), 0.2 (violet), 0.3 (blue), 0.4 (cyan), 0.5 (green), and 0.6 (yellow, the lightest marginal line).

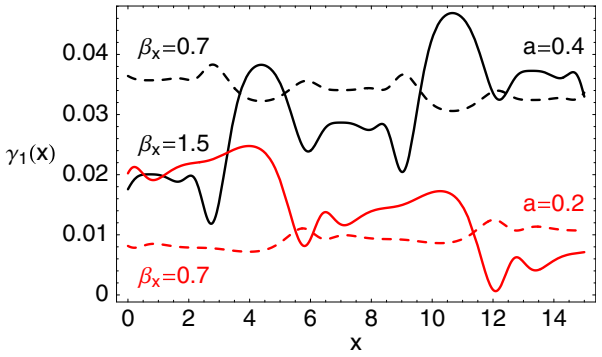

FIG. 2. The function $\gamma_1(x)$, Eq. (43) for $k(x)$ defined by Eq. (44) with $a = 0.2$ (red lower lines), $a = 0.4$ (black upper lines) and $\beta_x = 1.5$ (solid lines), $\beta_x = 0.7$ (dashed lines); $\beta_y = 1$ in all cases. The offset (integration constant) of $\gamma_1(x)$ is irrelevant.

driving the system in one direction along the x axis. We demonstrate it on a function

$$k(x) = (2 - \cos x)(1 + a\cos x - a\sin x), \tag{44}$$

depicted in Fig. 1 for various values of a. Motivation for our specific choice of $k(x)$ is rather technical. We want to show the symmetry breaking term in γ_1 in an analytic form and this function enables us to express the integral in Eq. (43) by a simpler formula, if compared, e.g., with the commonly used function $k(x) = k_0 + \sin x + \eta \sin 2x$. The crucial property of $k(x)$ is its asymmetry, controlled here by the parameter $a \in (0, 1/\sqrt{2})$; $a = 0$ represents the symmetric sinusoidal geometry and for $a > 1/\sqrt{2}$, $k(x)$ would become negative for some x.

To evaluate the integral in $\gamma_1(x)$ for our $k(x)$, it is advantageous to apply double integration by parts,

$$\begin{aligned}
\int \frac{k'^3}{k^4}dx &= -\frac{1}{3}\left(\frac{k'^2}{k^3} + \frac{k''}{k^2} - \int \frac{k^{(3)}}{k^2}dx\right),\\
\int \frac{k^{(3)}}{k^2}dx &= \tau_1(a)\arctan\left[\frac{a - (1-a)\tan(x/2)}{\sqrt{1-2a^2}}\right]\\
&\quad + \tau_2(a)\arctan\left[\sqrt{3}\tan\frac{x}{2}\right]\\
&\quad - \tau_3(a)\ln\left(\frac{1 + a\cos x - a\sin x}{2 - \cos x}\right)\\
&\quad - \frac{[\tau_4(a)(1+\cos x) - \tau_5(a)\sin x]}{(1 + 4a + 7a^2)^2(1 + a\cos x - a\sin x)}\\
&\quad + \frac{[\tau_6(a)(1+\cos x) - 18a(1-8a^2)\sin x]}{3(1 + 4a + 7a^2)^2(2 - \cos x)},
\end{aligned}$$

where the coefficients τ abbreviate

$$\begin{aligned}
\tau_1(a) &= 12a(1 - 4a - 54a^2 - 44a^3 + 190a^4 + 132a^5\\
&\quad - 285a^6 - 200a^7)(1 - 2a^2)^{-3/2}(1 + 4a + 7a^2)^{-3},\\
\tau_2(a) &= \frac{4a(5 - 23a - 276a^2 - 317a^3 + 179a^4)}{\sqrt{3}(1 + 4a + 7a^2)^3},\\
\tau_3(a) &= \frac{6a(1+a)(1+11a)(1-8a^2)}{(1 + 4a + 7a^2)^3},\\
\tau_4(a) &= \frac{2a^3(26 + 59a - 38a^2 - 91a^3 - 4a^4)}{(1-a)(1-2a^2)},\\
\tau_5(a) &= \frac{2a^2(7 + 23a - 6a^2 - 9a^3 - 19a^4 - 44a^5)}{(1-a)(1-2a^2)},\\
\tau_6(a) &= 1 + 18a + 105a^2 + 110a^3.
\end{aligned}$$

The terms with arctan give the nonzero increment of $\gamma_1(x)$ over the period $L = 2\pi$; subtracting its limits at π^- and $-\pi^+$,

$$\begin{aligned}
\Delta\gamma_1 &= \gamma_1(\pi - 0^+) - \gamma_1(-\pi + 0^+)\\
&= \frac{\pi\beta_x(\beta_x^2 - \beta_y^2)}{48\beta_y^4}[\tau_2(a) - \tau_1(a)].
\end{aligned} \tag{45}$$

Of course, $\gamma_1(x)$ remains analytic at $x = \pm\pi$. It continues risen by $\pm\Delta\gamma_1$ in the neighboring cells; see Fig. 2. The mean slope depends on asymmetry of $U(x, y)$, represented here by the parameter a. For the symmetric $k(x)$, $a = 0$, $\tau_1 = \tau_2 = \Delta\gamma_1 = 0$. Notice that the tilt of "teeth" in $k(x)$ inverts from the right to the left with growing a for our function Eq. (44); also the increment $\Delta\gamma_1$ changes from negative ($a = 0.2$) to positive ($a = 0.4$) for $\beta_x > \beta_y$. Exchanging the temperatures, the sign of $\Delta\gamma_1$ changes, too, according to Eq. (45).

The function $-\gamma_1(x)$ represents the first-order correction to an effective 1D potential $\sim -\ln A(x)$, which becomes increasing or decreasing on the scale of many periods L. It either cumulates the diffusing particles on one side until reaching the quasiequilibrium in general, $p_{\rm eq}(x) \sim A(x)$, or it drives a stationary flux J, Eq. (31). Describing the Feynman-Smoluchowski ratchet, the last case is applicable. The constant net flux J corresponds to the rotating ratchet wheel with averaged velocity $v = \Delta x/\Delta t = JL/N_c$; N_c is a normalization constant, corresponding to the number of particles in one cell of the channel for diffusion. The stationary 1D density $p_{st}(x)$ is obtained by solving Eq. (31) for a constant J. In the first order, $\hat{Z}_1$ is just a function (not containing ∂_x) and so the square bracket can be taken as the effective diffusion coefficient [16,17] $D(x) \simeq 1 - \epsilon\hat{Z}_1$. The solution is of the form

$$\frac{p_{\rm st}(x)}{A(x)} = e^{-\epsilon\gamma_1(x)}\frac{p_{\rm st}(x)}{A_0(x)} = \rho_0 - J\int_{x_0}^{x}\frac{e^{-\epsilon\gamma_1(x')}\,dx'}{A_0(x')D(x')}, \tag{46}$$

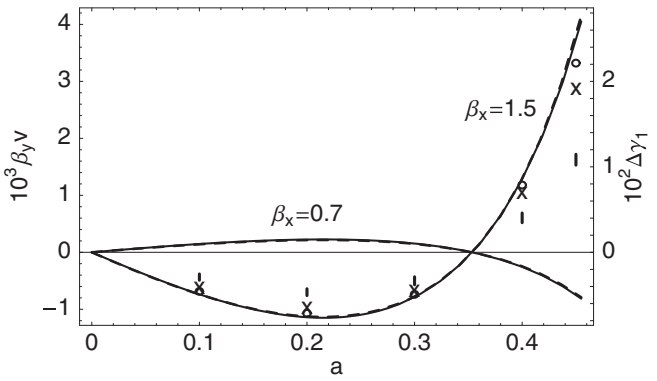

FIG. 3. Averaged velocity of the wheel, $v = JL/N_c$, scaled by the transverse inverse temperature β_y (solid lines, the left scale) depending on the parameter of asymmetry a for the temperatures $\beta_x = 0.7$ and 1.5; $\beta_y = 1$ and $\epsilon = 1$. The dashed lines (almost identical with the solid ones, the right scale) depict the increment of $\gamma_1(x)$ per one period, $\Delta\gamma_1$. The numerical solutions (using the algorithm of Ref. [4]) are depicted for $\beta_y = 1$ (vertical bars), 4 ("x"-es), and 10 (circles), keeping $\beta_x/\beta_y = 1.5$.

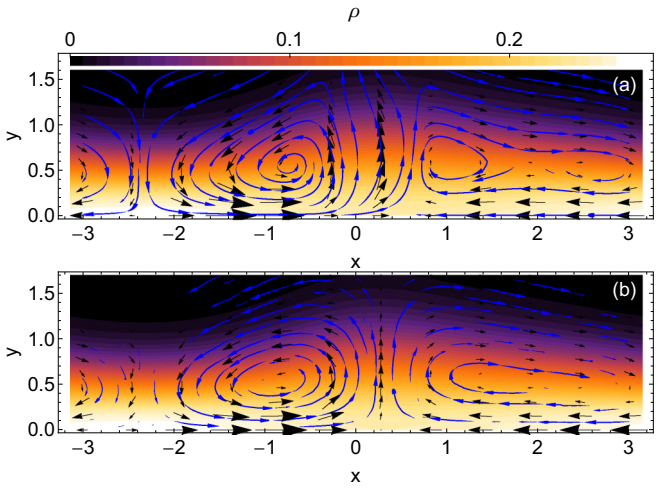

FIG. 4. Stationary density $\rho_{st}(x, y)$, (colors or gray levels) and the corresponding flux densities $\vec{j}_{st}(x, y)$ (streamlines) for $a = 0.2$, $\beta_x = 0.7$, $\beta_y = 1$, and $\epsilon = 1$. The size of the black arrows reflects magnitude of $\vec{j}_{st}$. Results of the backward mapping, Eq. (51) (panel a) are compared with the numerical solution (using COMSOL software) of the 2D problem for the same parameters (panel b).

x_0 denotes here some (arbitrary but fixed) reference point. The integration constant ρ_0, which is the averaged 2D density at $x = x_0$, is closely related to J. Requiring periodicity of the stationary density, $p_{st}(0) = p_{st}(L)$, we get

$$(1 - e^{-\epsilon\Delta\gamma_1})\rho_0 = J\int_0^L \frac{dx}{A_0(x)D(x)} e^{-\epsilon\gamma_1(x)}. \tag{47}$$

The normalization constant

$$N_c = \int_0^L \left[\rho_0 - J\int_0^x \frac{e^{-\epsilon\gamma_1(x')}\,dx'}{A_0(x')D(x')}\right] A_0(x)e^{\epsilon\gamma_1(x)}dx \tag{48}$$

set to unity fixes unambiguously solution of the problem. It expresses that the probability of finding the pawl and the wheel in any possible configuration within one period ("tooth") is 1. Eliminating ρ_0, using $\gamma_1(x + L) = \gamma_1(x) + \Delta\gamma_1$ and periodicity of $A_0(x)$, $D(x)$, Stratonovich's formula [18,19] generalized [20–25] by the varying effective diffusion coefficient $D(x)$ is obtained,

$$J = (1 - e^{-\epsilon\Delta\gamma_1}) \times \left[\int_0^L A_0(x)e^{\epsilon\gamma_1(x)}dx \int_x^{x+L} \frac{e^{-\epsilon\gamma_1(x')}dx'}{A_0(x')D(x')}\right]^{-1}. \tag{49}$$

The effective driving potential $\Delta\gamma_1$ (dashed lines) and the corresponding velocity of the wheel $v = 2\pi J$ (solid lines), calculated from our theory and depending on the parameter of asymmetry a, are plotted in Fig. 3. The scaling parameter ϵ is ratio of the real diffusion constants D_x/D_y of the wheel and pawl here (not only an auxiliary parameter), but we take $\epsilon = 1$ without studying technical properties of the ratchet device. The plots of the velocity and $\Delta\gamma_1$ versus a are almost identical after scaling by an appropriate multiplication factor. We can define an effective driving force F_{ef} connected with $\Delta\gamma_1 = F_{ef}L$; then $v = \mu_{ef}F_{ef}$, where the effective mobility μ_{ef} is well approximated by the (zeroth-order) Lifson-Jackson formula [26],

$$\mu_{ef} = \left[\frac{1}{L^2}\int_0^L A_0(x)dx \int_0^L \frac{dx}{A_0(x)D(x)}\right]^{-1}. \tag{50}$$

Our mapping procedure also enables us to reconstruct the 2D picture of the stationary state. Using the backward projection Eq. (22) up to the first-order Eq. (41), applied to $p_{st}(x)/A(x)$, Eq. (46), we obtain the formula for the corresponding 2D stationary density,

$$\rho_{st}(x, y) = e^{-G(x,y)}[1 + \epsilon\tilde{\omega}_1(x, y)\partial_x + \epsilon\omega(x, y)]\frac{p_{st}(x)}{A(x)}. \tag{51}$$

The flux density $\vec{j} = (j_x, j_y)$ is calculated by substituting Eq. (51) for ρ in the definition relations Eq. (8). Figure 4(a) shows the stationary regime for $\beta_x/\beta_y = T_y/T_x = 0.7$ and $a = 0.2$. The probability density ρ_{st} is depicted by colors or gray levels, and the streamlines and arrows describe the corresponding fluxes. The results are compared with the numerical solution of the full 2D problem, using the software package COMSOL, Fig. 4(b). We see that even the first-order (leading) terms give a relevant picture, describing the essence of the ratchet effect. The different temperatures $T_x \neq T_y$ give rise to a nonzero vortex force w, Eq. (35). It drives a couple of whirls, rotating in opposite directions in the narrowing and the widening part of one cell. The whirls are different because of asymmetry of the teeth, i.e., the spring constant $k(x)$, what results finally in a nonzero net flux J.

Regardless of a considerable agreement of the pictures obtained from Eq. (51) and the numerical solution in Fig. 4, the calculation and comparison of the ratchet effect obtained by both methods is a delicate task. The component j_x of the flux density as a function of y, plotted for several values of

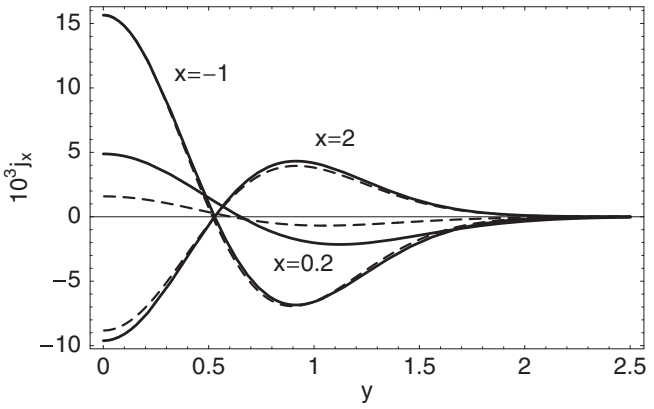

FIG. 5. The x component of flux density $j_x(x, y)$ for several values of x; $a = 0.2$, $\beta_x = 0.7$. The full lines come from Eq. (51), the dashed lines depict the numerical solution. The corresponding net flux $J = 3.565\times10^{-5}$ for any x.

x in Fig. 5, gives the integral J close to zero; the net flux J is only a tiny part of the fluxes flowing in the whirls. So the numerical solution requires us to compute ρ and its derivative j_x with maximum precision. At this point, we found that the algorithm developed by Ryabov *et al.* [4] is more effective for this specific task than the universal solver of the COMSOL package. Therefore, it was used for calculation of the numerical data in Fig. 3.

However, the results of the mapping, based on Eq. (51), represent only the leading terms, the first-order correction of the FJ Eq. (3). Small discrepancies between Figs. 4(a) and 4(b), caused by neglecting of the higher-order corrections in $p_{\rm st}$ and $\rho_{\rm st}$, are well visible in Fig. 5. The plots of j_x obtained from Eq. (51) (solid lines) differ from the numerical data (dashed lines) especially in between the neighboring whirls, e.g., at $x = 0.2$. Taking only the first order explains the difference between the theoretical velocity for $\beta_x = 1.5$ (solid line) in Fig. 3 and the numerical results (vertical bars) for the same parameters. Increasing $\beta_y > 1$ and holding the same ratio β_x/β_y has the same effect as taking the scaling parameter $\epsilon = 1/\beta_y < 1$; see Eqs. (43) and (45). The neglected higher orders become less important and the numerical values of velocity v multiplied by β_y approaches the theoretical line with growing β_y, see the crosses ($\beta_y = 4$, $\beta_x = 6$) and the circles ($\beta_y = 10$, $\beta_x = 15$) in Fig. 3. The higher-order corrections γ_n, necessary to achieve a better agreement, can be systematically derived by a straightforward although laborious extension of the theory introduced in Ref. [11].

The picture obtained within our analysis is in a qualitative agreement with the numerical study [27] of a more realistic potential of the ratchet. The lower boundary was shaped by a periodic function $h(x) > 0$ and the interaction of the pawl and wheel was described by the potential

$$U(x, y) = \frac{\lambda}{y - h(x)} + F_p y, \tag{52}$$

considering their repulsion in a thin contact layer of thickness $\sim\lambda$, F_p is a constant force pushing the pawl to the wheel. Expressing $f = -\beta_x \partial_x U$, $g = -\beta_y \partial_y U$ and using Eq. (18), we find the vortex force

$$w(x, y) = (\beta_x - \beta_y)\frac{\lambda h'(x)}{[y - h(x)]^2}, \tag{53}$$

calculated from the reference distance $h_0 \to \infty$. Nonzero w drives asymmetric stationary circulating probability currents, given by asymmetry of $h(x)$, resulting finally in the rectified motion of the device. The general formalism, presented in the Sec. II, also enables us to formulate the 1D effective theory for such models of the ratchets. The problems with calculation of the effective driving potential $-\gamma_1(x)$ are only technical, to complete the integrals containing $\exp[-\beta_y U(x, y)]$ for the potentials like Eq. (52).

A common simple model of the ratchet device considers the spring constant $k(x) = k$ and the potential $U(x, y) = U(y)$ independent of x; with only the boundary at $y = h(x) > 0$ binding both degrees of freedom. It represents an interesting limit in our theory, where the potential $U(x, y)$ has to describe properly the hard-wall repulsion in the infinitesimal layer at the boundary. If, e.g., $\lambda \to 0$ in Eq. (52), the corresponding $w(x, y)$ becomes zero, resulting in no ratchet effect. It suggests that the details of doing the limit from soft to the hard wall are important. We leave the detailed study of this problem to the future work.

IV. CONCLUSION

The main aim of the present paper was to show that the Feynman-Smoluchowski ratchet can be understood as a diffusive system driven by a nonconservative driving force. The vortex force $w(x, y)$, Eq. (18), appears here nonzero due to different temperatures T_x and T_y of the reservoirs connected to the ratchet wheel and the pawl, respectively. It drives a couple of competing stationary whirls in the narrowing and widening part of the cell, corresponding to one tooth of the wheel. Due to asymmetry of the potential landscape $U(x, y)$, the whirls differ from one another and the final net flow J, related to the velocity of the ratchet v, results as a net effect gained at the interface of the whirls.

We demonstrated that the 1D description offers an effective tool to study such phenomena. Mapping of the full-dimensional problem onto the longitudinal coordinate x, corresponding to the angle of the rotating wheel, leads again to the generalized Fick-Jacobs equation, Eq. (4). Unlike the previous mapped diffusive systems, the function $A(x)$ here is dependent on the scaling parameter ϵ, too. So the related 1D effective (real + entropic) potential $U_{\rm ef}(x) \sim -\ln A(x)$ can be expanded in ϵ; its coefficients $-\gamma_n(x)$ are calculated recursively together with the operators of backward mapping $\hat{\omega}_n(x, y, \partial_x)$ and the corrections to the FJ equation $\hat{Z}_n(x, \partial_x)$. As we demonstrated on the first-order coefficient $\gamma_1(x)$, Eq. (43), for $U(x, y) = k(x)y^2$ (Ryabov's model [4,5]), these corrections to the effective potential can break the periodicity of the system and give a nonzero increment of energy $\Delta\gamma$ per one period L. The original periodic potential becomes a slanted washboard potential in the 1D description; the effective driving force $F_{\rm ef} = \Delta\gamma/L$ drives the system (wheel) in one direction with velocity $v = \mu_{\rm ef} F_{\rm ef}$, Eq. (50), which is observed as the ratchet effect.

The 1D effective description enables us to handle the Feynman-Smoluchowski ratchet as any diffusive system driven by an external driving force. The presented calculation of F_{ef} and the corresponding velocity v was done here only up to the first order, so the results may deflect from the numerical values for some parameters of the model. Still, the mapping procedure, fully described in Ref. [11] can give the corrections to the force $\Delta\gamma_n/L$ up to any order $\sim\epsilon^n$. The future task may include the higher orders to an approximative formula, improving our first-order calculation and making the results applicable to a wider range of parameters of the model.

ACKNOWLEDGMENT

The work was supported by the Grant Agency of the Czech Republic, Grant No. 17-06716S and the Slovak VEGA Grant No. 2/0008/18.

[1] M. Smoluchowski, Phys. Z. **13**, 1069 (1912).
[2] P. Reimann, Phys. Rep. **361**, 57 (2002).
[3] R. P. Feynman, R. B. Leighton, and M. Sands, *The Feynman Lectures on Physics* (Addison-Wesley, Boston, 1963), Vol. 1.
[4] A. Ryabov, V. Holubec, M. H. Yaghoubi, M. Varga, M. E. Foulaadvand, and P. Chvosta, J. Stat. Mech. (2016) 093202.
[5] V. Holubec, A. Ryabov, M. H. Yaghoubi, M. Varga, A. Khodaee, M. E. Foulaadvand, and P. Chvosta, Entropy **19**, 119 (2017).
[6] P. Kalinay and J. K. Percus, J. Chem. Phys. **122**, 204701 (2005).
[7] P. Kalinay and J. K. Percus, J. Stat. Phys. **123**, 1059 (2006).
[8] P. Kalinay and J. K. Percus, Phys. Rev. E **74**, 041203 (2006).
[9] P. Kalinay and J. K. Percus, Phys. Rev. E **83**, 031109 (2011)
[10] S. Martens, G. Schmid, L. Schimansky-Geier, and P. Hänggi, Phys. Rev. E **83**, 051135 (2011); Chaos **21**, 047518 (2011).
[11] P. Kalinay and F. Slanina, J. Phys.: Condens. Matter **30**, 244002 (2018).
[12] M. H. Jacobs, *Diffusion Processes* (Springer, Berlin, 1967).
[13] S. Martens, A. V. Straube, G. Schmid, L. Schimansky-Geier, and P. Hänggi, Phys. Rev. Lett. **110**, 010601 (2013).
[14] S. Martens, G. Schmid, A. V. Straube, L. Schimansky-Geier, and P. Hänggi, Eur. Phys. J. Spec. Top. **222**, 2453 (2013).
[15] F. Slanina, Phys. Rev. E **94**, 042610 (2016).
[16] R. Zwanzig, J. Phys. Chem. **96**, 3926 (1992).
[17] D. Reguera and J. M. Rubí, Phys. Rev. E **64**, 061106 (2001).
[18] R. L. Stratonovich, Radiotekh. Elektron. **3**, 497 (1958).
[19] P. Reimann, C. Van den Broeck, H. Linke, P. Hänggi, J. M. Rubí, and A. Pérez-Madrid, Phys. Rev. E **65**, 031104 (2002); Phy. Rev. Lett. **87**, 010602 (2001).
[20] D. Reguera, G. Schmid, P. S. Burada, J. M. Rubí, P. Reimann, and P. Hänggi, Phys. Rev. Lett. **96**, 130603 (2006).
[21] P. S. Burada, G. Schmid, D. Reguera, J. M. Rubí, and P. Hänggi, Phys. Rev. E **75**, 051111 (2007)
[22] P. S. Burada, G. Schmid, P. Talkner, P. Hänggi, D. Reguera, and J. M. Rubí, Biosystems **93**, 16 (2008).
[23] P. S. Burada, P. Hänggi, F. Marchesoni, G. Schmid, and P. Talkner, Chem. Phys. Chem. **10**, 45 (2009).
[24] P. Kalinay, Phys. Rev. E **80**, 031106 (2009).
[25] P. Kalinay, J. Chem. Phys. **142**, 014106 (2015).
[26] S. Lifson and L. J. Jackson, J. Chem. Phys. **36**, 2410 (1962).
[27] M. O. Magnasco and G. Stolovitzky, J. Stat. Phys. **93**, 615 (1998).